Electrochimica Acta, 1971, Vol. 16, pp. 1663 to 1670. Pergamon Press. Printed in Northern Ireland

HYDROGEN EVOLUTION AND DISSOLUTION ON GRAPHITE ELECTRODES IN THE ELECTROLYSIS OF MOLTEN $KHSO_4$— I. KINETICS OF THE REACTIONS ON DENSE GRAPHITE*

E. J. BALSKUS, J. J. PODESTÁ and A. J. ARVÍA
División Electroquímica, Instituto Superior de Investigaciones, Facultad de Ciencias Exactas, Universidad Nacional de La Plata, La Plata, Argentina

Abstract—The kinetic parameters obtained under steady and non-steady conditions for cathodic hydrogen evolution and anodic hydrogen dissolution on dense graphite electrodes with molten potassium bisulphate at different temperatures are reported. The anodic E/i curves exhibit a 1/2 power dependence on hydrogen gas pressure. These results will be compared to those obtained with porous graphite electrodes in Part II of the present research, in an attempt to establish the probable mechanisms of the electrode processes.

Résumé—On donne les paramètres cinétiques obtenus dans des conditions stationnaires et non-stationnaires pour le dégagement cathodique et la dissolution anodique d'hydrogène sur des électrodes de graphite dense dans du bisulphate de potassium fondu à diverses températures. Les courbes de polarisation montrent une dépendence avec la racine de la pression d'hydrogène. Ces résultats seront comparés avec ceux qui s'obtiennent avec des électrodes de graphite poreux dans la deuxième partie de ce travail dans le but d'établir le mécanisme de réaction probable.

Zusammenfassung—Es werden kinetische Parameter für die kathodische Wasserstoffentwicklung und anodische Wasserstofflösung mitgeteilt, wie sie unter stationären und nichtstationären Bedingungen bei verschiedenen Temperaturen an dichten Graphitelektroden mit geschmolzenem Kaliumbisulfat erhalten wurden. Die anodische E/i-Kurve zeigt eine Wurzelabhängigkeit vom Wasserstoffdruck. Die Ergebnisse werden verglichen mit jenen, die an porösen Graphitelektroden erhalten wurden und in Teil II der vorliegenden Arbeit mitgeteilt sind. Es wird der Versuch gemacht, einen wahrscheinlichen Mechanismus der Elektrodenprozesse aufzustellen.

INTRODUCTION

THE HYDROGEN-evolution and -dissolution reactions in molten bisulphate have been the subject of systematic investigation in this laboratory in an attempt to get a sounder knowledge of their kinetics and probable reaction pathways. Thus, the reactions were studied in detail on different kinds of platinum electrodes,[1,2] on gold,[3] on palladium,[4] and iron electrodes,[5] and some qualitative information was also derived for other metals such as mercury, nickel and cobalt.[6]

The main conclusion of these researches is that, as in the case of aqueous solutions, the electrode reactions over rather a large range of potential are predominantly under activation control, and consequently these processes can be dealt with formally in the same way as in the case of acid aqueous solutions.

The present work, presented in two parts, extends the study of the kinetics and mechanism of the hydrogen electrode in bisulphate melts to the case of various kinds of graphite electrodes. Besides its interest from the point of view of fundamental electrochemistry, this study is also of importance for the application of graphite electrodes in fuel cell with melts, involving either the reduction of hydrogen ion or the oxidation of hydrogen gas.

EXPERIMENTAL TECHNIQUE

The cell employed in the experiments with dense graphite was essentially the same as that already described in the previous studies with electrodes of different

*Manuscript received 21 April 1970.

materials. The working electrodes consisted of graphite rods 6 mm in diameter with a spectroscopic graphite rod (National) of the same diameter and 2·5 cm long, inserted at right angle in one end of the rod. The electrochemically active area, as shown in Fig. 1, was a circle of 6 mm diameter, as the rest of the piece was electrically isolated by means of a boron nitride cover. The latter was obtained by repeated painting of the electrode surface with an aqueous suspension of boron nitride, a

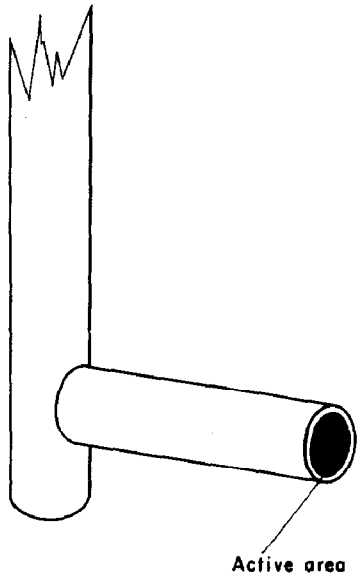

FIG. 1. Detail of the graphite working electrode.

previous drying of the piece at room temperature and a final drying at 240°C. The working electrode was polished with the finest degree emery paper and cleansed with sulphuric acid solution. This procedure gave a well defined and reproducible electrode surface of 0·28 cm^2 apparent area.

The counter-electrode was a platinum wire of large surface placed into a separate electrolytic compartment. A silver/silver(I) 3×10^{-2} M electrode, obtained by adding dried silver sulphate to the melt, was used as reference. The latter was mounted with the usual Luggin–Haber capillary tip arrangement.

Potassium bisulphate (AR Mallinckrodt and Riedel de Häen) and silver sulphate (Analar) were employed as molten electrolytes.

Different purified gases, such as hydrogen, nitrogen and oxygen were employed in the experiments. The purification procedure of the former gases was the same as that already described elsewhere.[7] Oxygen was purified in the conventional way.

The preparation of mixtures of hydrogen and nitrogen in different proportions was performed with the purified gases by means of a large glass container where the amount of each gas was evaluated manometrically. The gas mixture, which was dried at liquid-air temperature, was forced through the melt by water displacement.

Conventional anodic and cathodic galvanostatic and potentiostatic E/i curves were obtained by running the experiments under a controlled atmosphere.

Non-steady measurements were also performed to obtain either the galvanostatic build-up of overvoltage or its decay after interruption of the electrolysis current.

Anodic and cathodic voltammetric E/i curves were obtained by sweeping the applied electrode potential at different sweep rates.

Experiments with dense graphite electrodes were performed in the temperature range from 239–277°C.

RESULTS AND INTERPRETATION

1. *Cathodic steady* E/i *curves*

Galvanostatic E/i curves were obtained either with a freshly polished graphite surface or with graphite surfaces used repeatedly during various cathodic runs. All these experiments were done under hydrogen saturation of the melt at atmospheric pressure. Typical cathodic E/i curves obtained in these experiments are plotted semilogarithmically in Fig. 2. The E/i curves were well reproducible when the

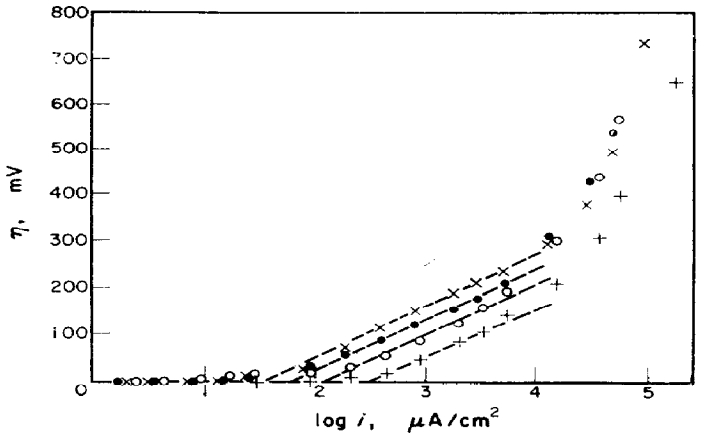

FIG. 2. Galvanostatic cathodic η/log i plot.
×, 239; ●, 244; ○, 261; +, 277°C.

working electrode had been previously used as cathode. Therefore this treatment was always applied to the graphite electrodes prior to the runs. The electrode rest potential obtained after the cathodic pulse was approximately 0·200 V at 240°C. The overvoltage η is referred to this rest potential and the cd is defined in terms of the apparent electrode area.

The Tafel plots exhibit three well-defined regions. The first, at low overvoltages, shows a large current increase for a minor increase of potential. The second region, extending from $i = 9 \times 10^{-5}$ up to $i = 15 \times 10^{-2}$ A/cm², exhibits a good straight-line portion, involving a $(b_T)_c$ slope. The third region extends beyond 10^{-1} A/cm², and apparently a limiting cd is approached. Table 1 comprises the $(b_T)_c$ values

TABLE 1. KINETIC PARAMETERS DERIVED FROM CATHODIC TAFEL LINES

Temp °C	$(b_T)_c$ V	$i_0 \times 10^6$ A/cm²	2·303 (RT/F) V
230	0·076	28·8	0·095
245	0·086	57·5	0·098
261	0·096	120·1	0·101
277	0·104	276·0	0·105

derived from the E/log i curves, as well as the apparent exchange current density, i_0, obtained by extrapolation of the Tafel line to $\eta = 0$. The exchange cd increases with temperature and from an Arrhenius plot (Fig. 3) an apparent activation energy equal to 29 ± 5 kcal/mole was obtained. This figure, which is surprisingly high for the process in question, is interpreted later.[8]

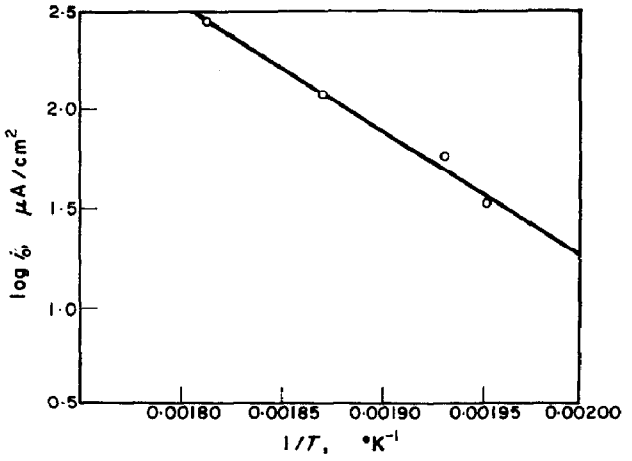

FIG. 3. Dependence of i_0 on temperature, according to an Arrhenius plot.

2. *Cathodic non-steady measurements*

The build-up and decay of cathodic overvoltage was recorded over a wide range of time. It was observed that the relaxation processes were rather slow and most of the records covered up to 10^3 s. The cathodic overvoltage after current interruption decayed logarithmically with time, as shown in Fig. 4. The decay slope, $(b_a)_c$, was between 0·050 and 0·070 V, as shown in Tables 2 and 3. From the cathodic decay

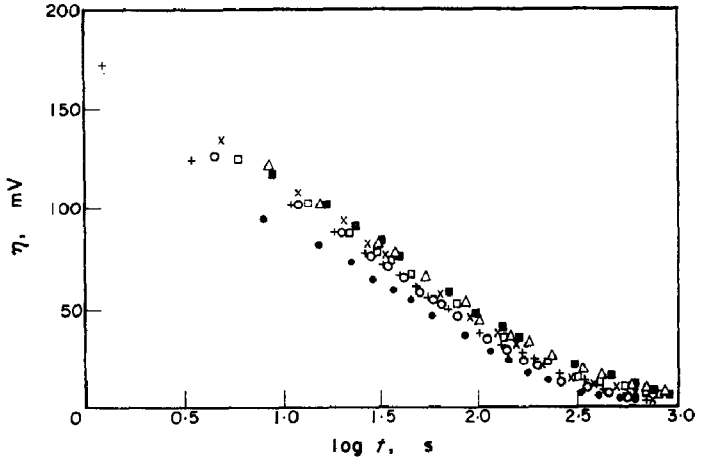

FIG. 4. Semilogarithmic plot of cathodic overvoltage decay at 278°C, after several cds. i: ●, 1564; +, 2661; ○, 4412; ×, 8775; □, 13,163; Δ, 16,684; ■, 20,948 μA/cm².

TABLE 2. KINETIC PARAMETERS DERIVED FROM CATHODIC OVERVOLTAGE DECAY. 262°C

η mV	$(b_a)_c$ V	t' s	$C_e \times 10$ F/cm²
85	0·045	7·60	1·45
132	0·052	1·33	0·95
157	0·052	0·477	0·60
180	0·052	0·210	0·44

TABLE 3. KINETIC PARAMETERS DERIVED FROM CATHODIC OVERVOLTAGE DECAY. 278°C

η mV	$(b_a)_c$ V	t' s	$C_e \times 10$ F/cm²
56	0·033	8·71	2·31
127	0·061	2·88	1·63
157	0·069	1·74	1·57
178	0·070	0·987	1·44
227	0·071	0·247	0·70
254	0·069	0·084	0·37
279	0·069	0·046	0·26
302	0·069	0·021	0·15

curves the apparent electrode differential capacitance, C_e, was evaluated. These figures are assembled in Tables 2 and 3; they decrease as the overvoltage increases. Values of C_e reported in the Tables are affected by a roughness factor of 2×10^2. Furthermore, the apparent electrode differential capacitances have a strong dependence on temperature.

3. *Anodic* E/i *curves*

The anodic *E/i* curves were obtained with recently polished electrodes without the previous treatment by electrical pulses. These experiments were run with hydrogen-gas saturation at different pressures. The corresponding hydrogen–nitrogen mixture saturated the melt for about 30 min before the experiments were run. Figure 5 shows typical galvanostatic runs. *E/i* curves are characterized by a

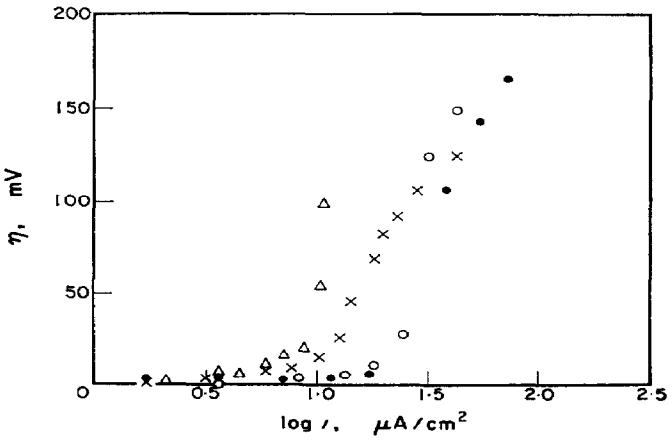

FIG. 5. Galvanostatic anodic η/log i plot at different hydrogen gas pressures, 240°C. p_{H_2}: ○, 1; ●, 0·5; ×, 0·27; △, 0·19 atm.

net anodic limiting current which gives a fairly acceptable linear increase with the square root of the hydrogen gas pressure, as displayed in Fig. 6. Results obtained from the anodic E/i curves are assembled in Table 4.

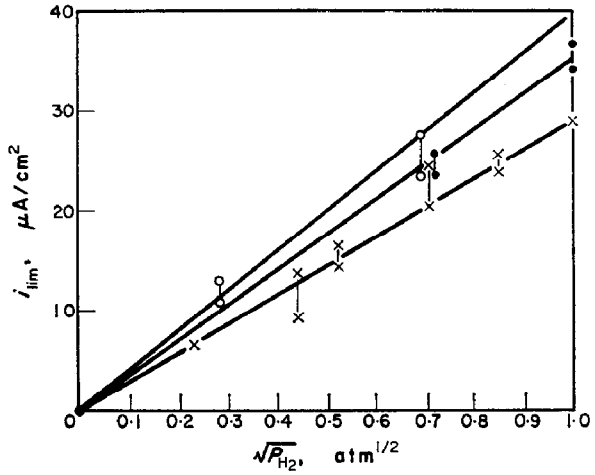

FIG. 6. Dependence of the galvanostatic anodic limiting cd on the square root of hydrogen-gas pressure.
×, 240; ●, 261; ○, 280°C.

TABLE 4. ANODIC LIMITING cds

Temp °C	p_{H_2} atm	$p_{H_2}^{1/2}$ atm$^{1/2}$	i_L μA/cm^2
240	0·052	0·228	6·4
	0·19	0·44	8·9–12·6
	0·27	0·52	14·2–15·9
	0·725	0·851	23·7–24·4
	1	1	28·2
261	0·51	0·714	23·0–25·1
	1	1	33·6–36·2
280	0·077	0·277	10·6–12·4
	0·50	0·71	23·0–26·54

4. *Non-steady anodic experiments*

A very slow decay of the anodic overvoltage was recorded and no satisfactory η/log t nor t/log η plot could be obtained. The results lacked an acceptable reproducibility. It was noticed, however, that a η/log t plot of an anodic decay curve starting from any potential corresponding to the limiting cd approached an infinite slope. The latter was also the slope obtained from the steady anodic E/log i curves already mentioned.

5. *Linear sweep voltammetry*

By applying a voltage sweep of 14 mV/s, voltammetric E/i diagrams were obtained starting from the rest potential of the working electrode and turning it towards the anodic direction. As shown in Fig. 7, the steady voltammetric E/i curves exhibit two more or less defined peaks involving anodic currents and two more corresponding

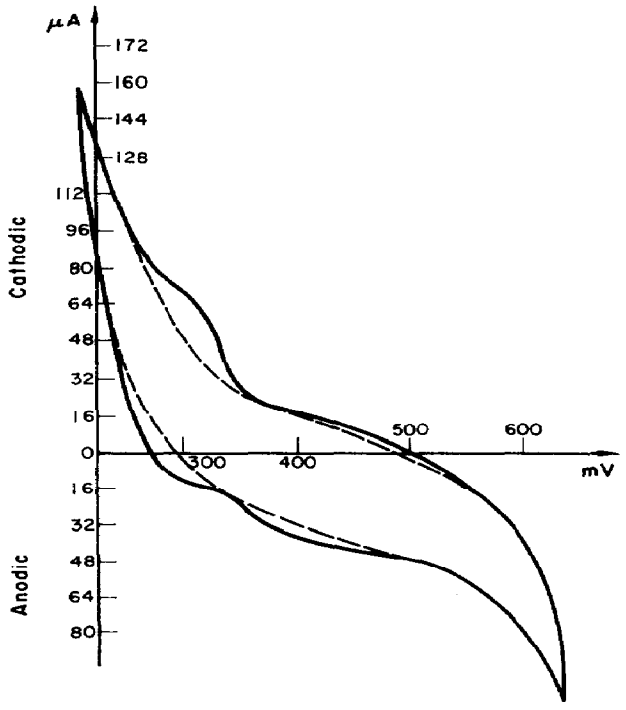

FIG. 7. Voltammetric current/potential curve.
250°C; sweep rate 14 mV/s. Curves are corrected from the noise of the record, and must be considered as average curves.

to cathodic currents when the electrode potential decreases. The latter peaks are located within the same potential region as the former.

The anodic peak located at less positive potentials and the cathodic one located at more negative potentials have their maxima at about 0·070–0·080 V above the rest potential of the working electrode. The remaining two peaks have their maxima located in the potential range of 0·160–0·180 V.

The different regions pointed out in the voltammetric E/i curves are directly comparable to steady E/i curves obtained under the same experimental conditions (hydrogen-gas partial pressure, temperature and electrode pre-treatment).

One immediately deduces that the peaks appearing at lower anodic overvoltage correspond to a potential region coinciding with that where the anodic limiting cd is found, or else, that the pair of peaks located at higher anodic overvoltages corresponds to the potential region where the electrochemical oxidation of bisulphate ion takes place. This reaction provokes the oxidation of graphite to CO and CO_2 and its kinetics and mechanism has been studied recently.[8] There is, therefore, a satisfactory coincidence between the results of steady and non-steady anodic measurements.

CONCLUSIONS

The kinetic study of electrochemical hydrogen evolution and dissolution on dense spectroscopic graphite, shows the occurrence of an activated electrode process,

which presents a more complex behaviour then that already discussed, for the same reactions on other electrode materials.[1–6]

A straightforward mechanistic interpretation of the reactions requires additional information. It appears particularly important to confirm the one-half power dependence of the anodic limiting cd on hydrogen pressure and to check the high figure already mentioned for the experimental activation energy of the cathodic reaction. For the purpose, these reactions were studied on a porous graphite electrode, and results are reported in Part II.[9]

Acknowledgements—This research was done under a U.S.A.F. Grant (AFOSR-69-1780) and with support of the Consejo Nacional de Investigaciones Científicas y Técnicas of Argentia. J. J. P. acted as a researcher of the Departamento de Ingeniería Química de la Universidad Nacional de La Plata.

REFERENCES

1. H. A. VIDELA and A. J. ARVÍA, *Electrochim. Acta* **10**, 21 (1965).
2. A. J. ARVÍA, A. J. CALANDRA and H. A. VIDELA, *Electrochim. Acta* **10**, 33 (1965).
3. A. J. ARVÍA, F. DE VEGA and H. A. VIDELA, *Electrochim. Acta* **13**, 581 (1968).
4. A. J. ARVÍA, A. J. CALANDRA and H. A. VIDELA, *Electrochim. Acta* **14**, 25 (1969).
5. R. CASINO, J. J. PODESTÁ and A. J. ARVÍA, *Electrochim. Acta* **16**, 121 (1971).
6. A. J. ARVÍA, A. J. CALANDRA and H. A. VIDELA, *An. Asoc. quím. argent.* **54**, 143 (1966).
7. D. GILROY and J. E. O. MAYNE, *J. appl. Chem.* **12**, 382 (1962).
8. A. J. ARVÍA, W. E. TRIACA and H. A. VIDELA, *Electrochim. Acta*, **15**, 9 (1970).
9. E. J. BALSKUS, W. E. TRIACA and A. J. ARVÍA, *Electrochim. Acta*, in press.